



Published in final edited form as:

Integr Biol (Camb). 2016 February 15; 8(2): 149–155. doi:10.1039/c5ib00265f.

Capillary Plexuses are Vulnerable to Neutrophil Extracellular Traps

Leo Boneschanker^{†,a,b}, Yoshitaka Inoue^{†,a}, Rahmi Oklu^c, and Daniel Irimia^{a,d}

^aBioMEMS Resource Center, Department of Surgery, Massachusetts General Hospital, Harvard Medical School, Shriners Burns Hospital, Boston, MA 02129

^bTransplant Research Program, Boston Children's Hospital, Boston, MA 02115

^cDepartment of Interventional Radiology, Massachusetts General Hospital, Harvard Medical School, Boston, MA 02129 (current address: Division of Interventional Radiology, Mayo Clinic, Scottsdale, AZ 85258)

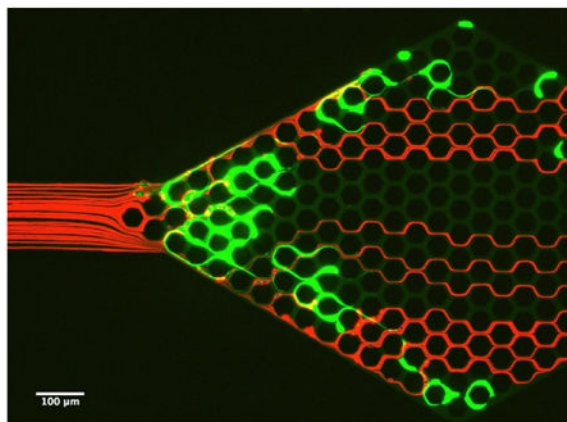
Abstract

Capillary plexuses are commonly regarded as reliable networks for blood flow and robust oxygen delivery to hypoxia sensitive tissues. They have high levels of redundancy to assure adequate blood supply after when one or more of the capillaries in the network are blocked by a clot. However, despite having extensive capillary plexuses, many vital organs are often subject to secondary organ injury in patients with severe inflammation. Recent studies have suggested that neutrophils play a role in this pathology, even though their precise contribution remains elusive. Here we investigate the effect of chromatin fibres released from overly-activated neutrophils (neutrophil extracellular traps, NETs) on the flow of blood through microfluidic networks of channels replicating geometrical features of capillary plexuses. In an *in vitro* setting, we show that NETs can decouple the traffic of red blood cells from that of plasma in microfluidic networks. The effect is astonishingly disproportionate, with NETs from less than 200 neutrophils resulting in more than half of a 0.6 mm² microfluidic network to become void of red blood cell traffic. Importantly, the NETs are able to perturb the blood flow in capillary networks despite the presence of anti-coagulants. If verified to occur *in vivo*, this finding could represent a novel mechanism for tissue hypoxia and secondary organ injury during severe inflammation in patients already receiving antithrombotic and anticoagulant therapies.

Graphical abstract

^dPlease address correspondence to: dirimia@hms.harvard.edu.

[†]equal contributions.



We show that the trapping of neutrophil-derived chromatin fibres at the entrance of microchannel networks *in vitro* can result in the formation of disproportionately large areas with no RBC traffic.

Introduction

A continuous traffic of red blood cells (RBCs) through capillaries delivers the oxygen necessary to cells in tissues. Perturbation of RBC traffic in capillaries, by extrinsic compression or intrinsic blockage, can result in tissue hypoxia, dysfunction, and damage. Preventing such situations, networks of interconnected capillaries in anatomical capillary plexuses provide redundancy of blood flow paths. Even when some capillaries are blocked, capillary plexuses assure adequate supply of RBCs to all tissue areas. However, vital organs that possess robust capillary plexuses are often damaged during inflammatory processes that take place in distant parts of the body.¹ Despite extensive research efforts, the mechanisms of remote injury remain poorly understood.² Elucidation of these mechanisms may lead to new strategies for prevention and management of inflammation, improve patient outcomes and decrease morbidity and mortality.

A role for neutrophils in tissue hypoxia and secondary organ damage during systemic inflammation has emerged from studies in animal models, which showed that removal of the neutrophils from the circulation protects against secondary organ injury.³⁻⁵ Recently, the release of chromatin from neutrophils, in the form of neutrophil extracellular traps (NETs) has come under scrutiny.⁶ NETs can activate platelets and catalyze the formation of small platelet aggregates *in vitro*.^{7, 8} *In vivo*, NETs entangled with platelets and RBCs have been identified at the core of venous thrombi, suggestive for a role in vascular pathology.⁹ Furthermore, elevated plasma DNA levels have been associated with increased risk for deep venous thrombosis¹⁰ and acute myocardial infarction.¹¹ However, therapies targeting the activation of platelets and coagulation factors in these conditions had limited efficacy in the clinic.^{12, 13} Alternative explanations for how neutrophils contribute to the damage of vital organs in the absence of thrombus formation have to be considered.

Here we provide first evidence for the ability of NETs to mechanically perturb the flow of blood through micro-channel networks *in vitro*. Our findings support an emerging hypothesis asserting that capillary plexuses are highly vulnerable to mechanical

perturbations by chromatin fibres released from activated neutrophils, independent of thrombus formation and in the presence of anticoagulants. We show that the trapping of NETs released from a few hundred neutrophils at the entrance of microchannel networks can result in the formation of disproportionately large areas void of RBCs. The perturbation of RBC traffic can last longer than 30 minutes in the presence of blood and anticoagulants and is corrected promptly by enzymatic degradation of NETs.

Biophysics of Particle Flow around Solid and Permeable Obstacles

The flow of particles around obstacles depends on the fluid permeability of obstacles. Classical fluid mechanics predicts that when moving around solid obstacles, the particles remain on the original fluid lines before and after the obstacle (Fig. 1A). However, when interacting in flow with permeable obstacles, the trajectories of particles and fluid become decoupled.¹⁴ Particles are pushed to the side of the obstacle, on new flow lines, while the fluid passes through the obstacle.¹⁵ The disjunction of particles and fluid persists behind the obstacles. Because transversal forces to bring the particles back behind the obstacle are absent, large spaces behind permeable obstacles become void of particles (Fig. 1B).

The current dogma explaining the robustness of capillary networks to localized obstructions is based on the flow of particles around solid obstacles. Specifically, RBCs flowing around blocked capillaries would re-enter the capillaries behind the blockage, limiting the RBC-void areas to that of the blockage (Fig. 2A). Oxygen and nutrients will continue to be transported to all cells in the tissue outside the obstruction while CO₂ and waste products will be removed. In contrast to this situation, we predict that the presence of permeable obstacles inside capillary networks results in drastically different flow patterns. RBCs are diverted by the permeable obstacles and are prevented from re-entering in capillaries downstream by the presence of plasma flow. Areas void of RBC traffic can form behind the obstacles and have sizes significantly larger than that of the permeable obstacles (Fig. 2B). *In vivo*, the same processes may be responsible for ischemia, tissue damage, and organ injury.

Results

We probed the consequences of trapping chromatin fibres, released from overly-activated neutrophils (NETs), in capillary networks, *in vitro*. For this purpose, we employed microfluidic networks with hexagonal arrays of channels, with $10 \times 10 \mu\text{m}$ cross-section and $50 \mu\text{m}$ pitch, replicating a human peritubular capillary plexus.¹⁶ We stimulated human neutrophils to release the NETs upstream of the microfluidic capillary network. We used gentle flow to transport the NETs and trap these in capillary networks downstream. We noted that following trapping, NETs can stretch across the entrances of multiple channels in the network (Fig. 3A). Furthermore, we observed that the traffic patterns of RBCs are perturbed not just at the site of NETs trapping, but throughout the entire network, with large areas being void of RBC traffic (Fig. 3A). In control experiments, we observed complete filling by flowing RBCs of all the channels behind complete obstructions (Fig. 3B).

The chromatin released from ~200 human neutrophils after PMA activation could completely block the traffic of RBCs in areas larger than ~50% of the entire network

(average area $0.3 \pm 0.1 \text{ mm}^2$ - Fig. 4). The disproportion between the amount of chromatin trapped and the size of the areas of the network that were completely void of RBCs (Fig. 4B) is consistent with the fluid-particle disjunction around permeable obstacles. In control experiments, we instilled $10 \mu\text{l}$ of heparinized whole blood through the device and observed no NETs trapping in the device and no changes in RBC flow patterns (Fig. 4A, Supplementary Fig. 1), suggesting that NETs and not thrombi or large cells blocking channels are responsible for the observed perturbations of RBC flow.

We compared the trapping of NETs in capillaries of various sizes and found that smaller channels can trap NETs with higher efficiency. Two capillary networks in series serve to quantify the trapping of NETs in channel networks of various geometries. The NETs passing through the first network of capillaries are being trapped with high efficiency in the second network. We observed chromatin fibers as long as $400 \mu\text{m}$ to get trapped in the two networks of capillaries (Fig. 5A and Supplementary Fig. 2). This arrangement helps quantify the fraction of NETs being captured in the first network of channels with width between 10 and $50 \mu\text{m}$. We found that the fraction of NETs captured in orthogonal capillary networks increases with the decreasing capillary width, from 50% on $30 \mu\text{m}$ wide channels, up to 80% for $10 \mu\text{m}$ wide channels (Fig. 5B).

The perturbation of RBCs traffic in capillary networks by the NETs-mediated blood disjunction can last for hours. Despite the natural presence of DNases in blood, we observed less than 5% change in the total area of the regions void of RBC traffic after 30 minutes of whole blood flow (Fig. 6). The obstructions caused by NETs are dynamic, revealed by the change in blood flow patterns under flow conditions for 30 minutes without DNase are not identical. We also observed the effect of high-yield Turbo™ DNase on NETs. The Turbo™ DNase is reported to be one order of magnitude more effective at DNA degradation compared to traditional DNase I. In our experiments, the Turbo DNase was able to degrade $93 \pm 4\%$ of the chromatin within 30 minutes (Fig. 7A) and restore RBC traffic in $73 \pm 9\%$ of the network (Fig. 7B). The chromatin degraded by Turbo DNase was released in small fragments, of which less than 5% were trapped in downstream networks. These short fragments did not perturb RBC traffic downstream in any significant manner.

Discussion

We replicated the typical dimensions of capillary plexuses in microfluidic networks of channels and found that the trapping of NETs released from a few hundred neutrophils could perturb the RBC traffic through millimeter-sized networks. The effect of NETs is disproportionate compared to the size of the neutrophils, with areas of perturbed RBC traffic one order of magnitude larger than the size of the neutrophils releasing the NETs. The branching geometry of large capillary plexuses makes them vulnerable to obstruction by NETs and subsequent RBC traffic perturbations.

The *in vitro* model presented in this study enabled us to isolate the mechanical effect of NETs from the biochemical actions on platelets, coagulation factors, and endothelial cells. The mechanical effect of NETs on RBC traffic occurs in the presence of high concentrations of robust anticoagulants. Furthermore, the perturbation of blood flow by NETs is

independent of the previously described activation of platelets or coagulation cascade.^{7, 8} If validated *in vivo*, it will represent a novel mechanism of tissue hypoxia.

The potential clinical implications of NETs trapping in capillary plexuses can only be speculated at this time. Circulating blood *in vivo* passes through two sets of capillary networks every minute, once in tissues and once in the lungs. In these conditions, chromatin released from neutrophils activated in the lung (e.g. during severe pneumonia), may be transported by the arterial blood through the systemic circulation and be trapped in capillaries in the kidney. The proximal tubules cells, which have high metabolic needs and are next to the extensive branching of the peritubular capillary plexus are predicted by our model to be extremely vulnerable to local perturbations of RBC flow.¹⁷ This chain of events could explain the association between major burn injury and subsequent acute tubular necrosis and liver injury.¹⁸ In other conditions, the trapping of NETs in capillaries may have a beneficial effect. For example, chromatin released during inflammation in a tissue is likely to be transported to the lung, where it is mechanically trapped by the dense capillary network of the alveolae.¹⁹ In contrast to the capture of NETs in peripheral tissues however, the capture of NETs in alveolar capillaries has no consequences on the viability of lung epithelial cells, due to their proximity to air. Only during acute inflammation responses, when large amounts of NETs are released in the circulation at once, they may overload this natural filtration mechanism and eventually lead to respiratory distress.

Ameliorating the vulnerability of plexuses to the mechanical trapping of NETs will require new treatments to be considered, beyond the use anti-coagulation and thrombolytic therapies.¹² Our *in vitro* results indicate that the degradation of NETs by DNases in the blood samples from healthy volunteers requires significantly longer than 30 minutes, a duration that may be excessive and lead to irreversible tissue damage. The utility of DNase injected intravenously has been tested in some animal models of chronic disease.²⁰ However, the DNases available today may not be potent enough to re-establish RBC flow in capillaries promptly after acute events and before hypoxic tissue damage is irreversible. Therapeutic targets that prevent chromatin release from neutrophils and other cells may also be beneficial, in addition to faster and more potent DNases.

Experimental

Microfluidic devices were manufactured using standard microfabrication techniques. Briefly, one layer of 10 µm thick negative photoresist (SU8, Microchem, Newton, MA) was patterned on a silicon wafer by employing one photolithography mask. This wafer served as a mold to produce PDMS (Polydimethylsiloxane, Fisher Scientific, Fair Lawn, NJ) parts. After curing for at least 12 hours in an oven set to 65°C, the PDMS layer was peeled off and inlet and outlet holes were punched with a 0.75 mm puncher. Finally, the devices were bonded irreversibly to standard glass slides (75×25 mm, Fisher Scientific).

To isolate neutrophils, human peripheral blood samples from healthy volunteers, aged 21 years and older, were purchased from Research Blood Components, LLC (Allston, MA). Peripheral blood was collected in 10mL tubes containing either EDTA or sodium heparin (Vacutainer; Becton Dickinson). Nucleated cells were isolated using a HetaSep gradient,

followed by the EasySep™ Human Neutrophil Enrichment Kit (STEMCELL Technologies, Vancouver, Canada) according to the manufacturer's protocol. Neutrophils were stained with Hoechst 33342 dye (Life Technologies, Carlsbad, CA) according to the manufacturer's protocol and suspended in a buffer of 0.2% human serum albumin (HSA, Sigma-Aldrich, St. Louis, MO) in Hanks Buffered Salt Solution (HBSS, ATCC, Manassas, VA) for experiments.

For each experiment, between two and four hundred neutrophils suspended in a buffer of HBSS/HSA (0.2% HSA) were stimulated for 12 hours with 50 nM Phorbol 12-myristate 13-acetate (PMA, Sigma Aldrich) to release NETs inside the cell-loading area of the microfluidic device. To identify the NETs, 50 μ L HBSS/HSA buffer with 5 μ M Sytox green (Life Technologies, Grand Island, NY) was flushed slowly through the devices. NETs were identified at the original locations of neutrophils by Sytox green stains larger than 25 microns. After applying higher flow through the channel, the number of NETs released into the capillary network was calculated by the difference between the number of NETs in the cell loading area before and after the flush. The flow pushes the NETs towards the micro-capillary network downstream, where they are trapped. Chromatin trapping in the micro-capillaries was recorded using time-lapse imaging on a fully automated Nikon TiE microscope (10 \times magnification) with bio-chamber heated to 37°C with 5% carbon dioxide gas. The number of NETs trapped in the capillary arrays was counted and matched with the number of NETs that had been flushed out of the cell-loading channel. To quantify the efficiency of NETs trapping, the number of NETs produced and the number of NETs trapped in the second hexagonal network is counted and the difference used to calculate the efficiency of capture in the first capillary network.

Following NETs trapping in the micro-capillaries, fresh human blood was stained using CellMask™ orange plasma membrane dye (Life Technologies) and infused in the device using a syringe pump (Harvard apparatus, Holliston, MA) at 0.3 μ L/min flow rate. RBC flow patterns were analyzed using long exposure time or by stacking 50 fast time-lapse images at video rate and subtracting them from a minimum intensity image, stacked for maximal intensity, and then merged into a single image using NIS-Elements to visualize flow patterns.

To degrade chromatin fibres, cell culture media or blood, with or without Turbo™ DNase (4 Units per 100 μ L blood/media; Life Technologies) was introduced in the device through the inlet at a flow rate of 0.3 μ L/min. The degradation of trapped chromatin was recorded using time-lapse imaging. The area in the micro-capillary bed that stained positive for chromatin by Sytox green was measured using Image J and compared to the stained area after DNase infusion at several time points.

Image analysis was performed using NIS-Elements (Nikon Inc, Melville, NY) and Image J (NIH). We assessed the number of neutrophils releasing NETs and measured the area of micro-capillaries blocked by trapped NETs, as well as the area with impeded blood flow. Statistical analysis included the student t test for normally distributed data and one-way ANOVA with Tukey's Post Hoc test. To compare DNase activity over time we used two-way ANOVA repeated measure with Sidak's multiple comparisons test. Linear

regression analysis was performed using Graphpad Prism (Graphpad software Inc, La Jolla, CA). Differences were assumed to be statistically significant for $p < 0.05$.

Conclusions

We provide *in vitro* evidence for the ability of neutrophil-derived chromatin fibres (NETs) to mechanically perturb the blood flow through micro-channel networks *in vitro*, without the need of thrombi being present. We suggest that the trapping of NETs at the entrance of capillary networks *in vitro* can result in the formation of large areas with no RBC traffic. Further studies could help develop new strategies to prevent or degrade NETs, which would work in conjunction with current antithrombotic and anticoagulation therapies, and prevent secondary organ injury after inflammation.

Supplementary Material

Refer to Web version on PubMed Central for supplementary material.

Acknowledgments

This work was supported in part by the National Institutes of Health (grants no. AG051082, GM092804, and EB002503). LB was supported by training grant T32AI007529.

References

1. Cohen J, Vincent JL, Adhikari NK, Machado FR, Angus DC, Calandra T, Jaton K, Giulieri S, Delaloye J, Opal S, Tracey K, van der Poll T, Pelfrene E. *Lancet Infect Dis*. 2015; 15:581–614. [PubMed: 25932591]
2. Massberg S, Grahl L, von Bruehl ML, Manukyan D, Pfeiler S, Goosmann C, Brinkmann V, Lorenz M, Bidzhekov K, Khandagale AB, Konrad I, Kennerknecht E, Reges K, Holdenrieder S, Braun S, Reinhardt C, Spannagl M, Preissner KT, Engelmann B. *Nature medicine*. 2010; 16:887–896.
3. Brown KA, Brain SD, Pearson JD, Edgeworth JD, Lewis SM, Treacher DF. *Lancet*. 2006; 368:157–169. [PubMed: 16829300]
4. Awad AS, Rouse M, Huang L, Vergis AL, Reutershan J, Cathro HP, Linden J, Okusa MD. *Kidney international*. 2009; 75:689–698. [PubMed: 19129795]
5. Narasaraju T, Yang E, Samy RP, Ng HH, Poh WP, Liew AA, Phoon MC, van Rooijen N, Chow VT. *Am J Pathol*. 2011; 179:199–210. [PubMed: 21703402]
6. Brinkmann V, Reichard U, Goosmann C, Fauler B, Uhlemann Y, Weiss DS, Weinrauch Y, Zychlinsky A. *Science*. 2004; 303:1532–1535. [PubMed: 15001782]
7. von Bruhl ML, Stark K, Steinhart A, Chandraratne S, Konrad I, Lorenz M, Khandoga A, Tirniceriu A, Coletti R, Kollnberger M, Byrne RA, Laitinen I, Walch A, Brill A, Pfeiler S, Manukyan D, Braun S, Lange P, Riegger J, Ware J, Eckart A, Haidari S, Rudelius M, Schulz C, Echtler K, Brinkmann V, Schwaiger M, Preissner KT, Wagner DD, Mackman N, Engelmann B, Massberg S. *The Journal of experimental medicine*. 2012; 209:819–835. [PubMed: 22451716]
8. Fuchs TA, Brill A, Duerschmied D, Schatzberg D, Monestier M, Myers DD Jr, Wroblewski SK, Wakefield TW, Hartwig JH, Wagner DD. *Proceedings of the National Academy of Sciences of the United States of America*. 2010; 107:15880–15885. [PubMed: 20798043]
9. Brill A, Fuchs TA, Savchenko AS, Thomas GM, Martinod K, De Meyer SF, Bhandari AA, Wagner DD. *Journal of thrombosis and haemostasis : JTH*. 2012; 10:136–144. [PubMed: 22044575]
10. van Montfoort ML, Stephan F, Lauw MN, Hutten BA, Van Mierlo GJ, Solati S, Middeldorp S, Meijers JC, Zeerleder S. *Arteriosclerosis, thrombosis, and vascular biology*. 2013; 33:147–151.

11. Stakos DA, Kambas K, Konstantinidis T, Mitroulis I, Apostolidou E, Arelaki S, Tsironidou V, Giatromanolaki A, Skendros P, Konstantinides S, Ritis K. *Eur Heart J*. 2015; 36:1405–1414. [PubMed: 25660055]
12. Mega JL, Simon T. *Lancet*. 2015; 386:281–291. [PubMed: 25777662]
13. Heffner JE, Sahn SA, Repine JE. *Am Rev Respir Dis*. 1987; 135:482–492. [PubMed: 3813208]
14. Michalopoulou AC, Burganos VN, Payatakes AC. *AIChE Journal*. 1992; 38:1213–1228.
15. Ramon GZ, Huppert HE, Lister JR, Stone HA. *Phys Fluids*. 2013; 25
16. Kramann R, Humphreys BD. *Semin Nephrol*. 2014; 34:374–383. [PubMed: 25217266]
17. Kramann R, Tanaka M, Humphreys BD. *Journal of the American Society of Nephrology : JASN*. 2014; 25:1924–1931. [PubMed: 24652794]
18. Inoue Y, Yu YM, Kurihara T, Vasilyev A, Ibrahim A, Oklu R, Zhao G, Nair AV, Brown D, Fischman AJ, Tompkins RG, Irimia D. *Crit Care Med*. 2015; 1097/CCM.000000000001397
19. Abrams ST, Zhang N, Manson J, Liu T, Dart C, Baluwa F, Wang SS, Brohi K, Kipar A, Yu W, Wang G, Toh CH. *Am J Respir Crit Care Med*. 2013; 187:160–169. [PubMed: 23220920]
20. Wong SL, Demers M, Martinod K, Gallant M, Wang Y, Goldfine AB, Kahn CR, Wagner DD. *Nature medicine*. 2015; 21:815–819.

Innovation, Integration, Impact

We designed a series of microfluidic devices to analyze the effect that chromatin fibres (neutrophil extracellular traps, NETs) have on red blood cell (RBC) traffic through networks of channels replicating geometrical features of capillary plexuses. We found that NETs trapped at the entrance of channels decouple the traffic of RBCs from that of plasma and lead to the formation of large areas void of RBCs. This mechanical effect of NETs on capillary plexuses takes place despite the presence of anti-coagulants and, when validated *in vivo*, may represent a new mechanism that links inflammation to tissue hypoxia and organ injury.

Author Manuscript

Author Manuscript

Author Manuscript

Author Manuscript

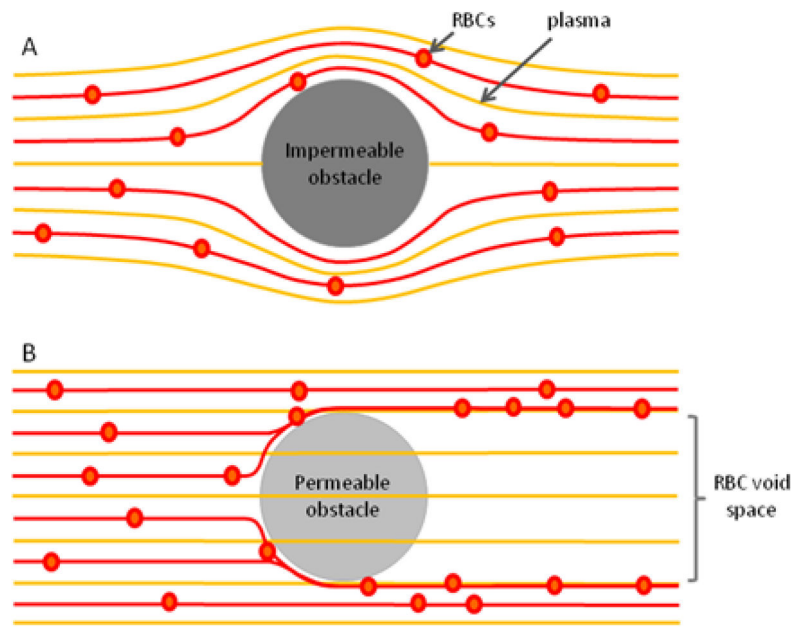


Figure 1. Particle and fluid flow around permeable and impermeable obstacles

A) Around impermeable obstacles, RBCs follow the fluid flow lines and the distribution of particles is the same before and after the obstacle. B) In contrast, only particles are deflected by permeable obstacles, while the fluid can go through unperturbed. After passing the obstacle, the particles remain in their flow line. As a result, a zone free of particles develops behind the permeable obstacle

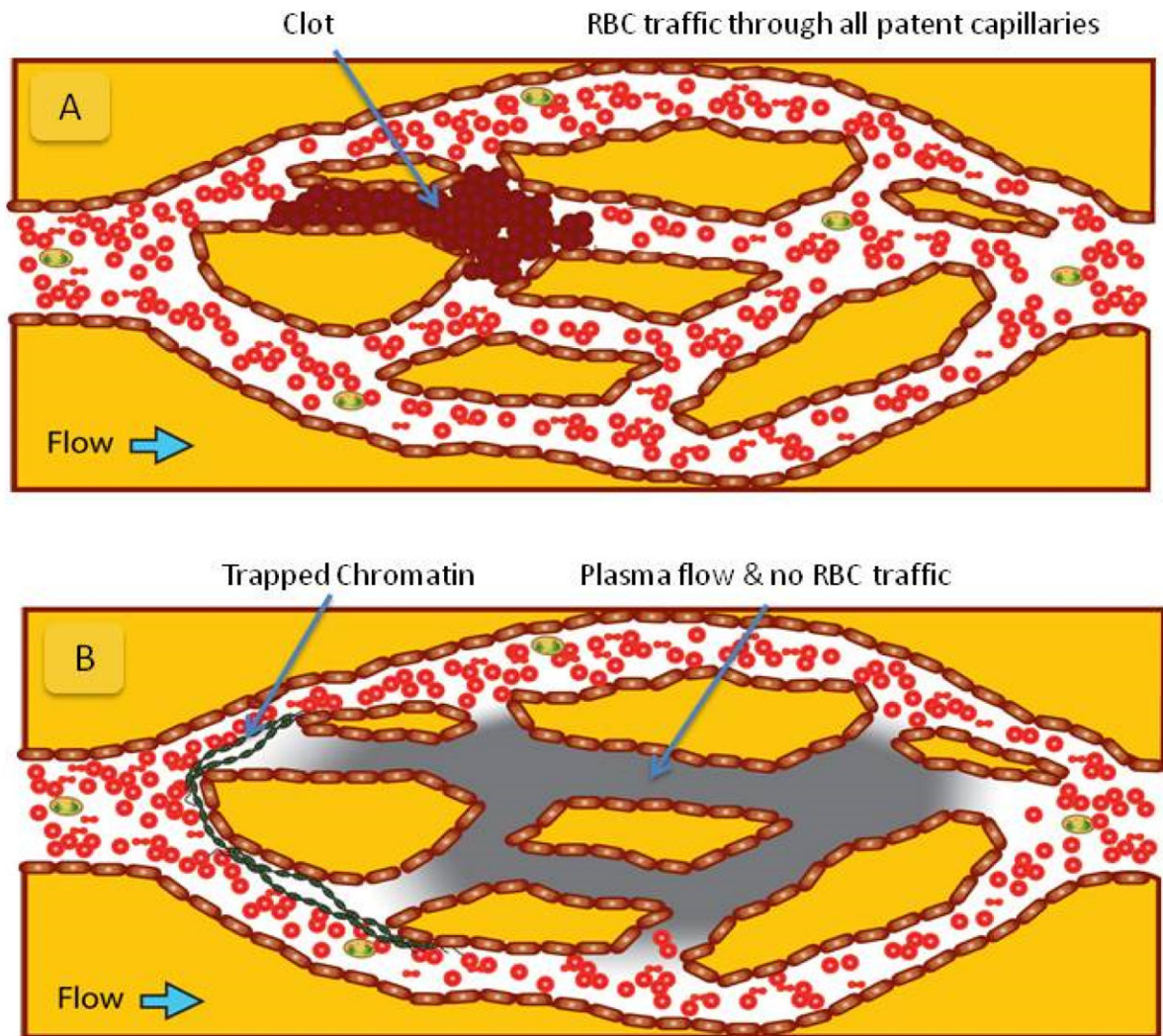


Figure 2. Capillary plexuses are vulnerable to chromatin trapping

Schematics of RBC and plasma flow in capillary networks with obstructions. A) Following complete blockage of a capillary by a clot (brown), plasma and RBC traffic is re-routed around the obstacles. RBCs fill all capillaries of the plexus behind the obstacle. B) Following chromatin trapping (green) at the entrance to the capillary plexus, the RBCs and plasma from whole blood are forced to take distinct paths through the network. Plasma can flow through the NETs obstacle while RBCs are mechanically diverted. In conditions of laminar flow, RBCs cannot reenter the plasma flow streams behind the obstacle and end up being completely excluded from large regions of the plexus. The size of the areas behind NETs that are RBC free is disproportionately large compared to the size and extension of the NETs.

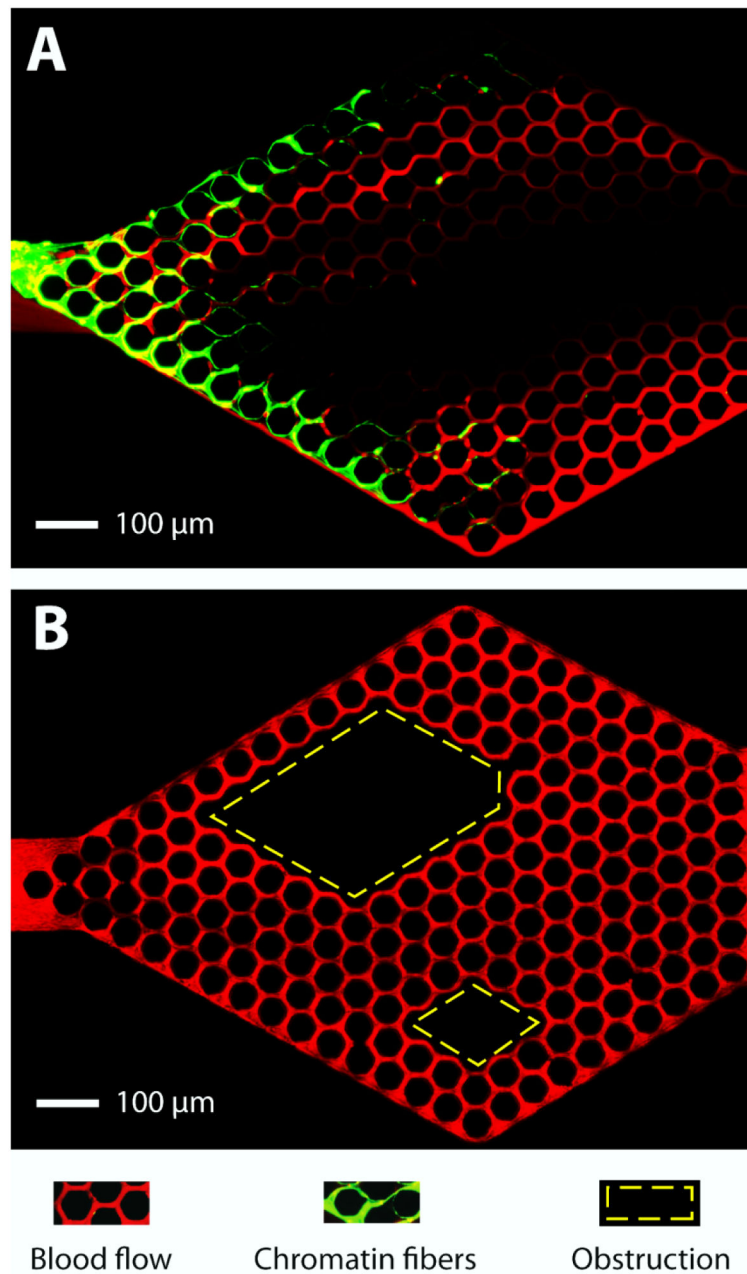


Figure 3. Trapped chromatin fibers perturb blood flow

A) NETs (green) released by the activation of human neutrophils upstream and trapped at the entrance of the capillary network, divert the traffic of RBCs (red) flowing through the device. An area void of RBCs extends from one end to the other of the capillary network. B) Whole blood flows through a capillary network with two large obstacles in the middle (rhomboidal areas outlined in yellow). Flow of RBCs through the network is maintained in all areas around and behind the obstacles. Flow is from left to right. The microfluidic devices consist of $10 \times 10 \mu\text{m}$ channels in a hexagonal pattern with $50 \mu\text{m}$ pitch. Scale bar represents $100 \mu\text{m}$.

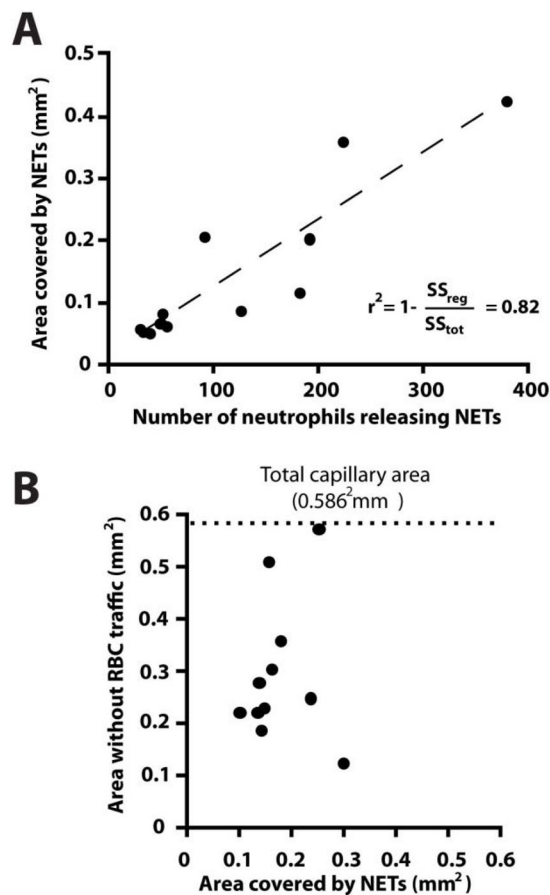


Figure 4. Chromatin trapping in hexagonal networks

A) The area covered by chromatin inside the network is proportional to the number of neutrophils that released chromatin upstream. **B)** The area with no RBC flow after chromatin release from ~200 neutrophils represents on average half of the total area of the network (0.30 ± 0.14 of the total 0.59 mm^2) and is larger than the area in which chromatin is trapped ($0.18 \pm 0.06 \text{ mm}^2$, $N=11$).

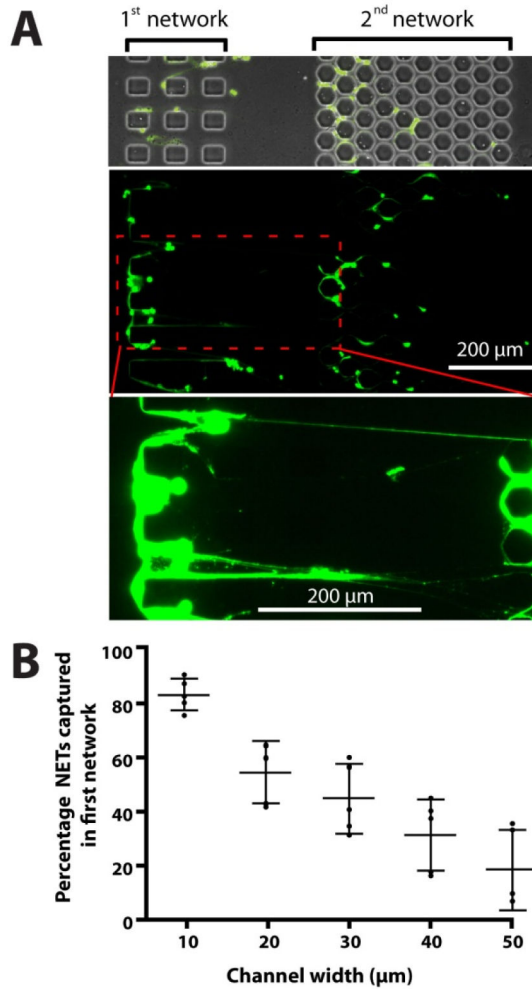


Figure 5. The fraction of NETs captured in the devices depends on the size of the channels

Two networks of channels are placed in series and the efficiency of chromatin capture as a function of channel size is evaluated by comparing the amounts of NETs trapped in each of the two networks. The width of channels in the first network ranges from 10 to 50 μm. The second network has 10 μm channels, captures NETs at better than 95% efficiency. The role of the second network is to help quantify the amount of NETs that escapes the first array of channels. All channels are 10 μm tall. Increased contrast shows chromatin fibers reaching lengths of over 400 μm. **B**) Smaller, 10 μm channels capture significantly more (~85 %) of the passing NETs than larger 40 μm channels (~30 % of the passing chromatin, $p < 0.05$). Bars represent mean ± standard deviation. Experiments representative of at least N=3 independent experiments.

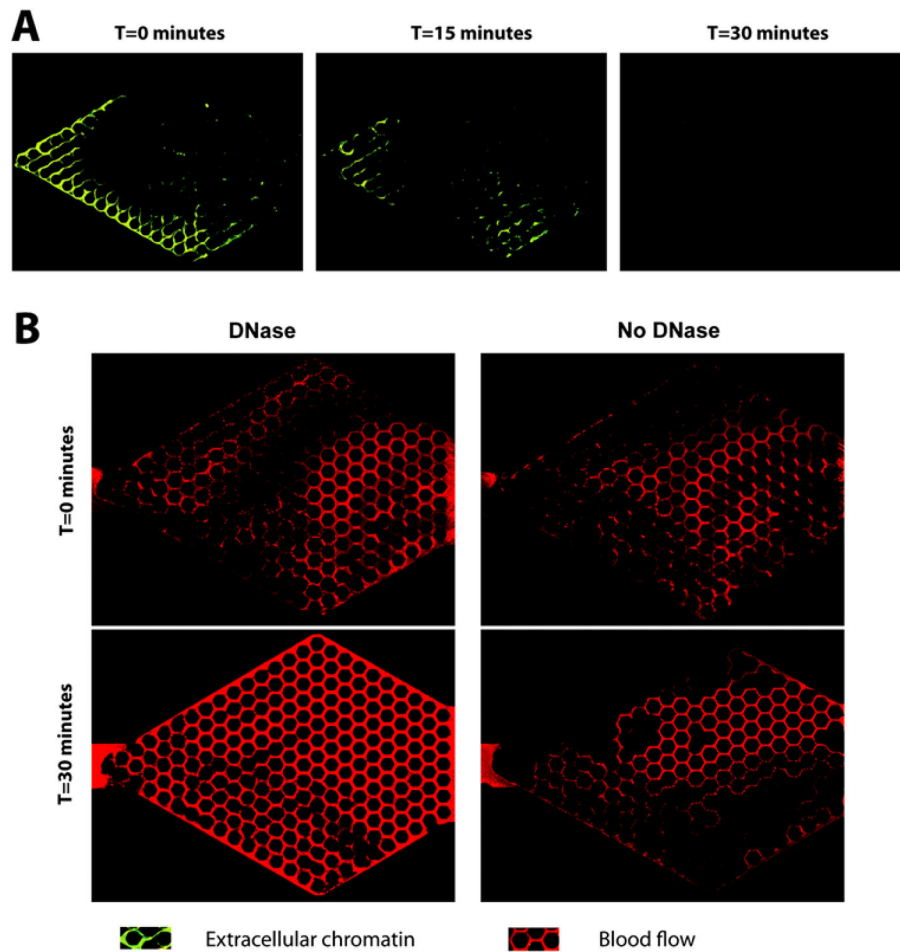


Figure 6. DNase degrades trapped chromatin and restores blood flow

A) DNase was incubated with the devices at 37°C for 30 minutes under flow conditions, resulting in the rapid breakdown of NETs and restoration of the blood flow. B) Trapped NETs significantly obstruct blood flow (top). Blood flow is restored within 30 minute following the infusion of DNase.

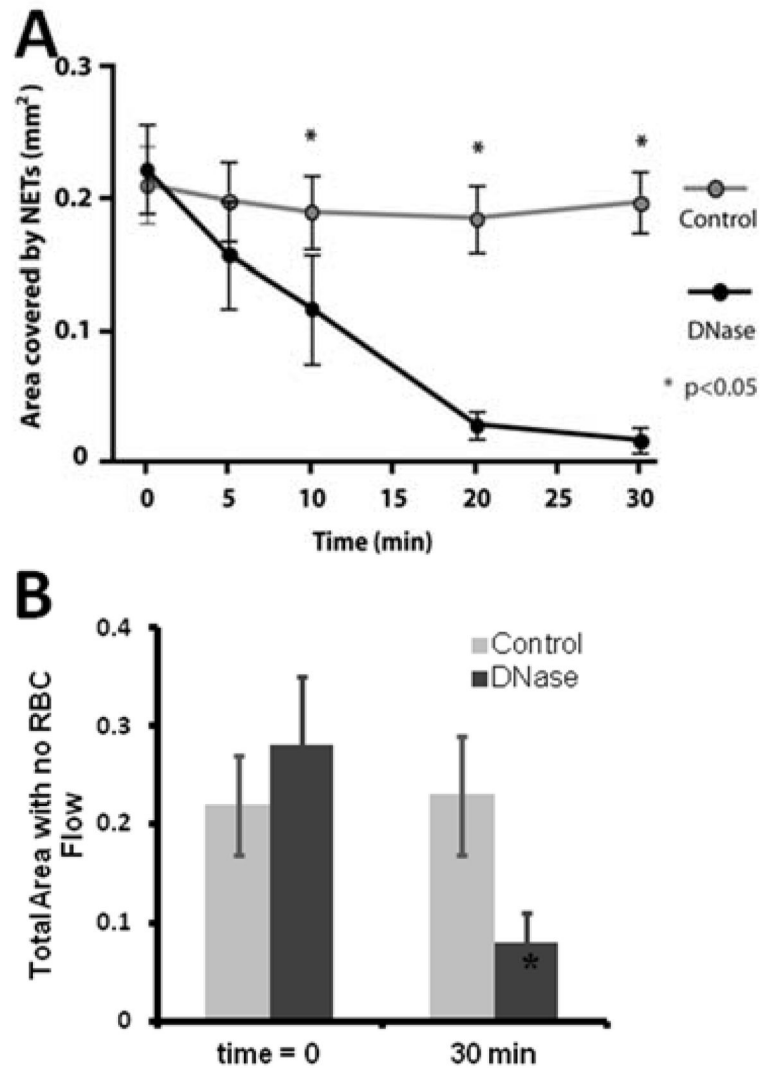


Figure 7. Chromatin degradation in the microfluidic network under flow

A) In control experiments, blood was infused at a constant rate of 0.3 $\mu\text{l}/\text{minute}$ for 30 minutes. In separate experiments, DNase was incubated with the devices at 37°C, for 30 minutes, followed by the injection of blood. The area covered by chromatin was analyzed 5, 10, 20 and 30 min after initiation of treatment. After 30 minutes, only $10.4 \pm 10\%$ of original chromatin was still present, significantly less than the whole blood control ($N=6$, $p<0.05$).

B) The area with no RBC flow behind the chromatin decreased to approximately one third of the initial area and $8 \pm 0.6\%$ of the total network area.